THE JOURNAL OF PHYSICAL CHEMISTRY C

Article

Cite This: J. Phys. Chem. C 2019, 123, 28969−28976

pubs.acs.org/JPCC

Metal-Ion-Induced Luminescence *Enhancement* in Protein Protected Gold Clusters

Jyoti Sarita Mohanty, Kamalesh Chaudhari, Chennu Sudhakar, and Thalappil Pradeep*

DST Unit of Nanoscience (DST UNS) and Thematic Unit of Excellence (TUE), Department of Chemistry, Indian Institute of Technology Madras, Chennai 600 036, India

Supporting Information

ABSTRACT: We probed the interaction between Au_{38}@BSA and various heavy metal ions using luminescence spectroscopy. Interestingly, Au_{38}@BSA showed luminescence *enhancement* upon interaction with Cd^{2+} and Pb^{2+} at concentrations higher than 1 ppm, due to the formation of cluster aggregates. Such aggregates were detected by dynamic light scattering (DLS) and high resolution electron microscopy (HRTEM) studies. Luminescence enhancement of Au_{38}@BSA in the presence of Cd^{2+} was due to the interaction of Cd^{2+} with the cluster core, while Pb^{2+}-induced luminescence enhancement was due to BSA-Pb^{2+} interaction. Observations were further supported by X-ray photoelectron spectroscopy (XPS) studies. This kind of phenomenon has been observed in protein protected clusters for the first time. We believe that such metal-ion-induced luminescence enhancement can be used to synthesize cluster systems with enhanced optical properties and different ion−cluster interactions can be used to develop metal ion sensors using Au_{38}@BSA.

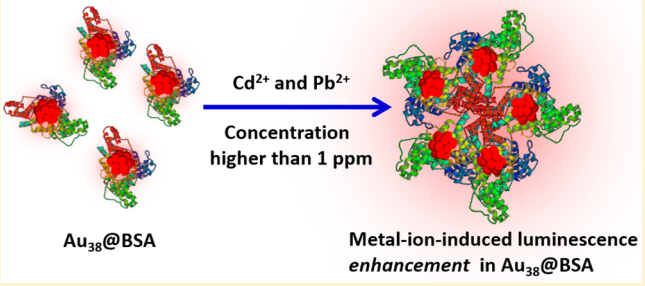

INTRODUCTION

The study of noble metal nanoclusters consisting of a few to hundred metal atoms has become fascinating due to their unique optical and electronic properties.[1−4] Especially, Au and Ag metal nanoclusters have been studied extensively due to their attractive optical properties. Such nanoclusters typically use thiols as protecting ligands, and various protocols in the solution phase[1] as well as solid state[5] have been developed for their synthesis. Macromolecular templates such as DNA,[6] dendrimers,[7] and most recently proteins,[3,8,9] have also been used for the synthesis of such nanoclusters. The most commonly used proteins are bovine serum albumin (BSA),[8,10−13] lysozyme (Lyz),[14−16] lactoferrin (Lf),[17,18] human serum albumin (HSA),[19,20] and a few others.[3,21] Protein protected noble metal clusters (PPCs) have been synthesized under basic pH and are stable over a wide pH range.[8,10,18] Typically the core of such nanoclusters is less than 2 nm in diameter. PPCs exhibit attractive optical, electronic, catalytic, and magnetic properties.[22] Luminescence of PPCs is stable under different pH conditions, and their quantum yield is high as compared to their monolayer protected counterparts. Due to the simple synthetic procedure and ease of modification with various functional groups, PPCs have been considered as major candidates for biolabeling, *in vivo* and *in vitro* imaging[13,23] and various sensing applications.[3,22] They are biocompatible due to lower metallic content and use of bulky proteins as ligands. High quantum yield and presence of various functionalities of PPCs can be used for highly selective and sensitive detection of analytes in various applications. Owing to their small size, biocompatibility, luminescence, and low toxicity, PPCs are good candidates for sensing of metal ions[24−26] and small molecules.[20,27−30]

Intense photoluminescence (PL) is one of the most interesting properties of PPCs. According to the previous reports, the reason for the high quantum yield of such clusters is FRET between the protein shell and the core of the cluster.[3,17] Recently, Chevrier et al. have studied the structural and intense luminescence properties of the BSA-stabilized gold cluster in detail.[31] It is also possible to tune the luminescence property of nanoclusters by changing the composition through alloying,[12] doping,[32] etc. Enhancement of luminescence through different routes has been studied by several groups. In our previous report, we have shown that an Au cluster protected by mixed proteins shows 3-fold enhancement in luminescence due to FRET.[33] Luo et al. have reported aggregation-induced luminescence enhancement of Au(I) thiolate where they have shown that the Au(I) thiolate shell surrounding the Au(0) core plays a role in enhancing the luminescence.[34] Metal-induced luminescence enhancement has been reported by Muhammed et al.,[13] where they found that the enhancement of luminescence in Au_{QC}@BSA was due to Ag nanoparticles where protein acts as a spacer between the gold cluster and the nanoparticles. A similar study has been demonstrated for glutathione-capped Au clusters by Ji et al.,

Received: August 2, 2019
Revised: October 29, 2019
Published: November 4, 2019

Downloaded via INDIAN INST OF TECH MADRAS on November 30, 2019 at 12:47:32 (UTC).
See https://pubs.acs.org/sharingguidelines for options on how to legitimately share published articles.

© 2019 American Chemical Society

DOI: 10.1021/acs.jpcc.9b07370
J. Phys. Chem. C 2019, 123, 28969−28976

where they have found that the enhancement was due to the formation of aggregates through GSH−Pb^{2+} interaction.[35] Exchanging the core with other metals can significantly change the luminescence property of a cluster as shown by Wang et al., where they observed drastic fluorescence enhancement in an Au cluster when it was doped with Ag atoms.[32]

It can be concluded from the above discussion that reactivity of clusters with metal ions can change their properties drastically. In particular, heavy metal ions can react with clusters in different ways, either with the core or with the protecting shell. Heavy metal ion contamination is one of the serious threats to human health and environment due to their toxic effects. Some of the heavy metals are biologically essential such as copper (Cu),[36] zinc (Zn),[37] and iron (Fe)[38] but at higher concentrations they can lead to toxicity while other heavy metals, namely, mercury (Hg),[39] cadmium (Cd),[40] and lead (Pb),[41] are not biologically essential, and their presence even at lower concentrations can cause harm to the organism.[42] Although various conventional analytical techniques have been used for analyzing metal ions,[43,44] PL spectroscopy is one of the simplest tools for such analysis.[13,24,25,45]

Due to strong surface plasmon resonance and its dependence on the surface protection, gold nanoparticles have been employed to detect heavy metal ions.[46,47] DNAzyme biosensors also showed good selectivity and sensitivity for detecting heavy metal ions.[48] PPCs are highly sensitive to the presence of specific metal ions and due to their high quantum yield, change in luminescence can be visualized with naked eyes and thus it can be an ideal candidate for sensing metal ions. Xie et al. have shown for the first time that BSA-stabilized Au clusters can be used for sensing Hg^{2+}, which quenches the luminescence of the former completely.[24] Sensing of Cu^{2+} ions in live cells using Au_{QC}@BSA has been reported by Durgadas et al.[49] Zeptomolar detection of explosives such as TNT and Hg^{2+} by using a hybrid material of Ag_{QC}@BSA and Au mesoflower has been shown by Mathew et al.[27] Goswami et al. have reported quenching of Pb^{2+} using Cu_{QC}@BSA.[45] Several other groups have also demonstrated sensing of various metal ions through luminescence quenching.[3,22]

Here in this paper, we report the luminescence *enhancement* in Au_{38}@BSA through metal-ion-induced aggregation. This phenomenon has been observed for the first time. It was found that Au_{38}@BSA forms aggregates when treated with higher concentrations of Cd^{2+} and Pb^{2+} which leads to a significant change in their luminescence property. The resulting aggregates were thoroughly characterized using various spectroscopic and microscopic techniques. The effect of Cd^{2+} and Pb^{2+} on Au_{38}@BSA has been studied in detail.

EXPERIMENTAL METHODS

Reagents and Materials. All the chemicals were commercially available and used without further purification. Bovine serum albumin (pH 6−7, SRL Chemical Co. Ltd., India), sodium hydroxide (RANKEM, India), tetrachloroauric acid trihydrate (CDH, India), $PbCl_2$ (CDH, India), $CdCl_2$ (CDH, India), $FeCl_2$ (CDH, India), $HgCl_2$ (Merck, India), $CuCl_2$ (Merck, India), and Sinapinic acid (Sigma-Aldrich) were used for the experiments. Triply distilled water was used for all the experiments.

Instrumentation. UV−vis spectra were collected using a PerkinElmer Lambda 25 spectrometer in the range of 200−1100 nm with a scan rate of 480 nm per minute. Luminescence measurements were carried out using a Jobin Yvon NanoLog spectrometer. For both excitation and emission, spectra were collected with a band-pass of 3 nm and the samples were excited at 365 nm. High resolution transmission electron microscopy (HRTEM) was performed with a JEOL 3010 instrument working at 300 kV, equipped with an ultra high resolution (UHR) polepiece. Energy dispersive X-ray analysis (EDS) was carried out with an Oxford EDAX housed in the TEM. Sample for HRTEM was prepared by dropping the dispersion on a carbon coated copper grid and drying under ambient conditions. MALDI MS study was conducted using an Applied Biosystems Voyager DE PRO Biospectrometry Workstation. A pulsed nitrogen laser of 337 nm was used for the studies and an average of 250 shots was used for each spectrum measurement. Sinapinic acid was used as the matrix for MALDI MS measurement. Dynamic light scattering (DLS) measurements were performed using a Malvern Zetasizer ZSP instrument. X-ray photoelectron spectroscopy (XPS) studies were carried out with an Omicron ESCA probe spectrometer with polychromatic Mg Kα X-rays ($h\nu$ = 1253.6 eV). The samples were spotted as drop cast films on a sample stub.

Synthesis. *Synthesis of Au_{QC}@BSA.* Au_{QC}@BSA was synthesized as reported previously.[8] In a typical synthesis, 1 mL of 6 mM tetrachloroauric acid trihydrate ($HAuCl_4{\cdot}3H_2O$) solution was added to 25 mg of BSA powder in 1 mL of distilled water, under vigorous stirring. The mixture was allowed to stir for 5 min. Then 100 μL of 1 M NaOH was added to the above mixture and stirred for 12 h until the solution turned golden brown in color. The reaction was carried out at room temperature. The solution of Au_{QC}@BSA was stored at 4 °C for further use.

Study of Interaction of Au_{38}@BSA with Different Metal Ions. For performing metal ion interaction studies with Au_{QC}@BSA, various metal ions such as Cd^{2+}, Pb^{2+}, Hg^{2+}, Fe^{2+}, and Cu^{2+} were chosen. Metal ion solutions of various concentrations were obtained by serial dilution of the stock solution. Typically, 5 μL of the cluster solution was diluted 400 times with distilled water. To study the interaction, different concentrations of metal ions were added to the above-mentioned cluster solution. After addition, the solution was mixed well and incubated for 2 min before recording the luminescence spectrum. It is well-known that Cu^{2+} and Hg^{2+} ions can quench the luminescence of Au_{QC}@BSA but the interaction of Au_{QC}@BSA with other metal ions has not been studied in detail. Therefore, from the perspective of toxic heavy metal ions, interactions of Cd^{2+} and Pb^{2+} were studied in detail.

RESULTS AND DISCUSSION

Spectroscopic and Microscopic Characterizations of Au_{QC}@BSA. Synthesis and characterization of gold cluster within BSA template was reported by Xie et al.[8] Briefly, the addition of $HAuCl_4.3H_2O$ to BSA forms Au^+−BSA complex. BSA contains 21 tyrosine residues which can reduce Au^{3+} to Au^+. Further reduction of Au^+ to Au^0 occurs by adding NaOH into the mixture. At alkaline pH, BSA acts both as a reducing and as a capping agent for Au cluster synthesis.[18] Due to the bulkiness of BSA, it provides steric protection to the cluster. Au_{QC}@BSA has been characterized using different spectroscopic and microscopic techniques (Figure 1), and the core of the cluster has been assigned using MALDI MS study (Figure S1).

DOI: 10.1021/acs.jpcc.9b07370
J. Phys. Chem. C 2019, 123, 28969−28976

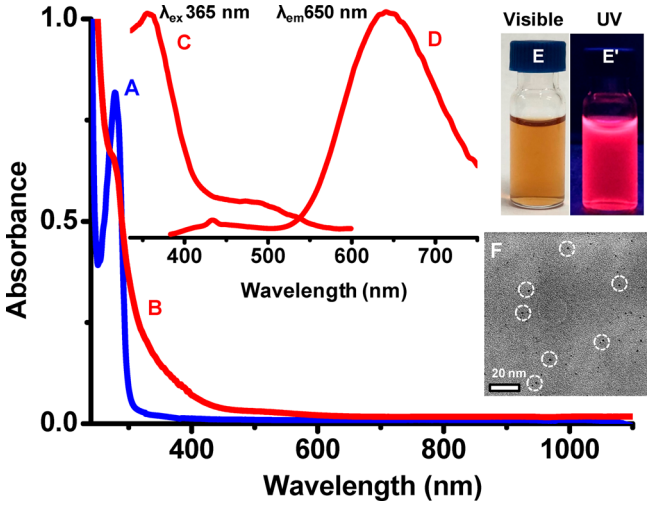

Figure 1. Comparison of UV−vis spectra for (A) pure BSA and (B) Au_{QC}@BSA. PL (C) excitation and (D) emission spectra of the cluster. The cluster shows an emission maximum at 645 nm and an excitation maximum at 365 nm. Inset shows the photograph of cluster solution under (E) visible and (E′) UV light. (F) HRTEM image of the sample shows a core size of around 1.8 nm. The clusters are shown with dotted circles. Scale bar in the HRTEM image is 20 nm.

A comparison between UV−vis absorption spectra for pure BSA and Au_{QC}@BSA is depicted in parts A and B of Figure 1, respectively. BSA shows an absorption feature at 280 nm due to the presence of aromatic amino acids such as tyrosine and tryptophan residues. In the case of Au_{QC}@BSA, a decrease in the absorption intensity at 280 nm was observed along with a shoulder at 375 nm as compared to that of pure BSA. The absence of a well-defined absorption feature in the case of clusters has been attributed to the encapsulation of the cluster by bulky BSA.[13] The PL excitation and emission spectra of the cluster are presented in parts C and D of Figure 1, respectively. Two excitation maxima around 365 and 500 nm were observed for the cluster as previously reported.[12] When the cluster was excited at 365 nm, two emission maxima, one around 450 nm which is due to weak luminescence from the protein and the other at 645 nm because of emission from the cluster, were found. The cluster showed bright red luminescence and photographs of the cluster under visible light and UV light are shown in Figure 1, parts E and E′, respectively. To study the size of clusters, HRTEM analysis was performed (Figure 1F). The core of the cluster was found to be below 2 nm, and no particles of bigger size were found. MALDI MS study was performed to assign the core of the cluster. The calculated mass difference between the parent protein and the cluster formed provides the number gold atoms present in the core of the cluster. Au_{QC}@BSA has a peak at m/z ~74 210 and the mass difference between Au_{QC}@BSA and BSA (m/z 66 700) was ~7.5 kDa, suggesting the formation of Au_{38}@BSA. So, henceforth Au_{QC}@BSA will be referred as Au_{38}@BSA.

With this background, our studies on the interaction of different metal ions with the cluster are discussed in the next section.

Metal-Induced Enhancement of Photoluminescence in Au_{38}@BSA. Clusters can interact with various metal ions through chemical functionalities of the protein or through the metal core. Interaction between different metal ions and clusters can bring changes in the PL as well as other properties of the cluster. Here, we have studied the effect of various metal ions such as Cd^{2+} and Pb^{2+} on the PL of Au_{38}@BSA. The emission spectra for Au_{38}@BSA and BSA in the presence of Cd^{2+} and Pb^{2+} ions at different concentrations are shown in Figure 2.

As shown in Figure 2A, different concentrations of Cd^{2+} were added to Au_{38}@BSA to monitor its effect on the luminescence profile. A decrease in the PL intensity was observed upon addition of 100 ppb Cd^{2+}. However, at 500 ppb, instead of further decrease, it leads to an *increase* in the PL intensity. Moreover, the addition of 1 ppm of Cd^{2+} resulted in higher emission intensity as compared to the parent cluster. With further increase in the concentration of Cd^{2+} from 1 to 10 ppm, luminescence intensity increased systematically. A gradual blue shift in the emission peaks from 650 to 630 nm was also noticed in the process, and when the concentration of Cd^{2+} reached at 10 ppm, it resulted in a ~2.7 fold enhancement of emission intensity. To find out the role of BSA on Cd^{2+} and Au_{38}@BSA interaction, similar concentrations of Cd^{2+} were added to BSA, and emission spectra were collected (Figure 2B). BSA showed an emission maximum ~ 335 nm when excited at 280 nm. At lower concentrations of Cd^{2+}, no change in the protein emission was noticed. Upon addition of increasing concentrations of Cd^{2+}, changes in the luminescence of BSA were less marked and were opposite to that of Au_{38}@BSA. Thus, it is suggested that PL enhancement in Au_{38}@BSA is due to the interaction of Cd^{2+} with the cluster core and not with the protein shell. Further studies with DLS and HRTEM were performed to understand the effect of Cd^{2+} on Au_{38}@BSA. These results are discussed in the next section of the paper.

Similar measurements were conducted to know the effect of Pb^{2+} on the PL properties of Au_{38}@BSA. Upon addition of 100 ppb of Pb^{2+}, a decrease in the PL intensity of Au_{38}@BSA was observed (Figure 2C) which was similar to that of Cd^{2+}. Further addition of Pb^{2+} (500 ppb to 10 ppm) resulted in a gradual increase in the luminescence intensity. Addition of 10 ppm Pb^{2+} caused a ~1.6 fold enhancement of the cluster. To understand the role of protein in this interaction, similar concentrations of Pb^{2+} were added to BSA. A systematic decrease in the protein emission was observed with increase in concentration of Pb^{2+} from 100 ppb to 10 ppm without any change in the position of emission. Pb^{2+} has a tendency to bind to proteins which could induce the aggregation of clusters through protein−protein interaction.[35] Such aggregation can result in aggregation-induced enhancement in luminescence. Although enhancement was observed in the presence of both the metal ions, Cd^{2+} showed a higher enhancement than Pb^{2+} at similar concentration, although reasons for enhancement could be different in both the cases. In the case of Cd^{2+}, major interaction was with the core and in the case of Pb^{2+}, major interaction was with the protein shell of the cluster. A shift in the cluster emission toward the blue region upon interaction with Cd^{2+} also suggests that the core itself is changing after interaction with Cd^{2+}. The calculated quantum yields for Au_{38}@BSA and Au_{38}@BSA in the presence of Pb^{2+} and Cd^{2+} were found to be 8.0%, 13.0% and 15.0%, respectively.

Control PL study was performed to check the sensitiveness of the incubation time (Figure S2A). Same parameters were maintained during each measurement. No enhancement in the emission intensity was observed in the parent cluster over time. During the course of time, no precipitates were seen either in the solution of parent cluster or in the presence of Pb^{2+} and Cd^{2+}. Time-dependent changes in I_{650} of Au_{38}@BSA upon

DOI: 10.1021/acs.jpcc.9b07370
J. Phys. Chem. C 2019, 123, 28969−28976

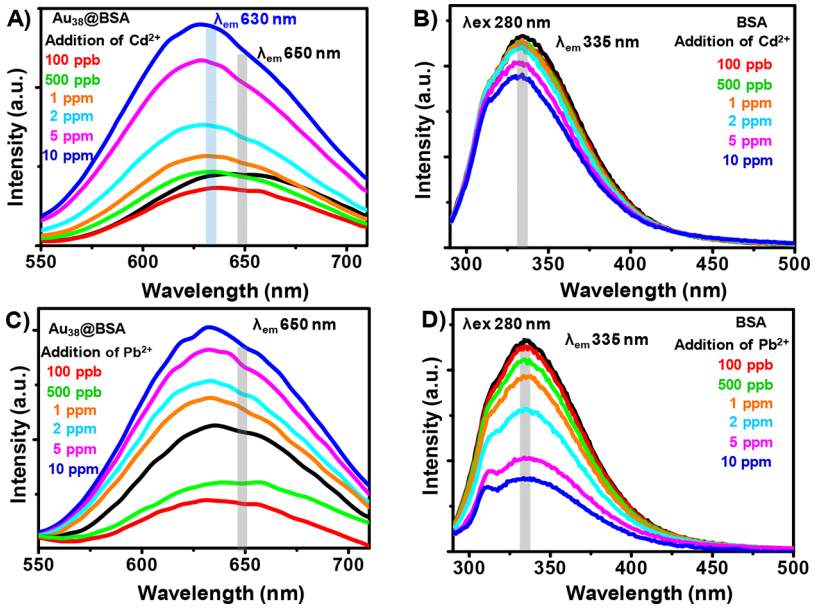

Figure 2. PL emission spectra of Au_{38}@BSA after treatment with (A) Cd^{2+} and (C) Pb^{2+}. The PL emission spectra of BSA after treatment with (B) Cd^{2+} and (D) Pb^{2+}. Excitation wavelengths for Au_{38}@BSA and BSA are 365 and 280 nm, respectively.

addition of 1 ppm concentration of Pb^{2+} and Cd^{2+} were measured to check the stability of the cluster. When Pb^{2+} (Figure S2B) and Cd^{2+} (Figure S2C) were added to the cluster solution, a large increase in I_{650} counts was observed, which was stable over long time. This suggested that the *enhancement* in emission intensity was due to the presence of Pb^{2+} and Cd^{2+}.

UV−vis absorption spectra of Au_{38}@BSA in the absence and presence of metal ions have been measured (Figure S3). As mentioned earlier, prominent absorption features were absent in protein protected gold clusters due to encapsulation by the bulky protein. The absorption peak at 280 nm is the characteristic feature of aromatic amino acids of the protein. No prominent change in the absorption features was seen upon adding Cd^{2+} to the cluster solution while a significant change was found upon Pb^{2+} addition. This change indicated that there is an interaction of Pb^{2+} with the protein shell of the cluster which also supports the PL studies.

Metal-Ion-Induced Aggregation Studies of Au_{38}@BSA by DLS and HRTEM. To investigate the effect of metal ions on the size of Au_{38}@BSA, DLS measurements were performed (Figure 3, parts A and B). From the DLS study, the size of BSA was found to be ∼ 7.6 nm and parent Au_{38}@BSA has a size of ∼ 9.7 nm, which are closely matching with the values reported (Figure S4).[50] This suggested that the cluster core to be of ∼ 2.1 nm and this value is slightly more than the size observed in HRTEM analysis (Figure 1F). The larger size observed in DLS measurement than by HRTEM is due to the presence of a solvation shell around the cluster in water. The volume fraction-dependent DLS measurement was carried out for the parent cluster. But no change in the size was observed with increase in concentration of the cluster (Figure S5). Figure 3A shows the changes in the size distributions of Au_{38}@BSA when different concentrations of Cd^{2+} were added to the former. Size of the cluster (9.7 nm) increased gradually upon interaction with increasing concentrations of Cd^{2+}, and finally, it reached ∼40 nm at 10 ppm of Cd^{2+}. Similar results were also obtained in the case of Pb^{2+} (Figure 3B) but at 10 ppm, it led to bigger aggregates of the clusters. Changes in the size of the parent cluster in the presence of Cd^{2+} and Pb^{2+} implied that the interaction of both the metal ions with the cluster induced their aggregation.

To further confirm the aggregation of the cluster, HRTEM analysis was performed at a higher concentration of metal ions (Figure 3, parts C, C′, D, and D′). TEM images of the clusters with Cd^{2+} are shown in Figure 3, parts C and C′. It clearly shows aggregation of the clusters. Similar aggregates were also found in the case of Pb^{2+} (Figure 3, parts D and D′). Compact aggregation of clusters was seen in this case (Figure 3D). These aggregates are mostly spherical in shape. Magnified image of one such spherical aggregate is shown in Figure 3D′. In both the cases, sizes of the clusters are much larger than the parent one (Figure 1F). This result confirms the metal-ion-induced aggregation of the cluster. The presence of Cd^{2+} and Pb^{2+} has been confirmed by EDS analyses (Figures S6 and S7).

XPS Studies of Au_{38}@BSA in the Presence of $Cd^{2+}$and Pb^{2+}. X-ray photoelectron spectroscopy (XPS) is an important tool to reveal the oxidation states of elements in the sample. XPS analysis of parent Au_{38}@BSA has shown that Au $4f_{7/2}$ appears at 84.1 eV, confirming the presence of a stable metallic core (Au^0 state) in the cluster (Figure S8A).[17] The binding energy of S $2p_{3/2}$ at 162.1 eV suggested Au−S bonding which stabilizes the core through cysteine residues of the protein (Figure S8B). The PL data shown in Figure 2 proposed that the major interaction of Cd^{2+} is with the core of the cluster whereas Pb^{2+} interacts with the BSA shell of the cluster. To further investigate metal-ion-induced changes in the oxidation states of cluster core and interacting elements, we carried out XPS analysis of Au_{38}@BSA upon interaction with Cd^{2+} and Pb^{2+} (Figure 4).

Due to the interaction of Cd^{2+}, Au $4f_{7/2}$ at 84.1 eV got shifted to 85.3 eV suggesting the oxidation of the core to Au^{1+}. However, two peaks at 406.4 and 404.6 eV binding energy were seen in the Cd 3d region and assigned as Cd^{2+} and Cd^0, respectively. After interaction with Pb^{2+}, only a change of 0.4 eV in the binding energy of Au $4f_{7/2}$ was observed (from 84.1 to 84.5 eV), indicating the core to be closer to its metallic state, and the binding energy at 138.9 eV was the characteristic feature of Pb^{2+}. The XPS data have shown that Cd^{2+} induced a

DOI: 10.1021/acs.jpcc.9b07370
J. Phys. Chem. C 2019, 123, 28969−28976

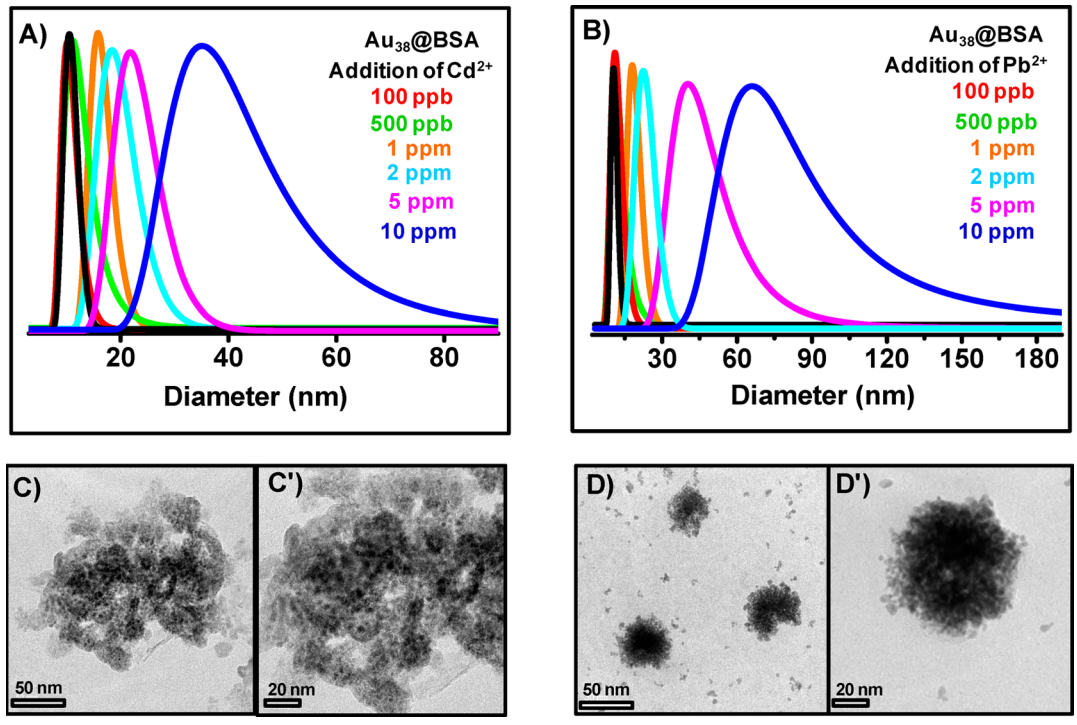

Figure 3. DLS spectra of Au_{38}@BSA at various concentrations of (A) Cd^{2+} and (B) Pb^{2+}. Data for parent Au_{38}@BSA are also shown. TEM images showing the aggregation of clusters upon adding (C) Cd^{2+} and (D) Pb^{2+}. The corresponding higher magnification TEM images are shown in parts C′ and D′, respectively.

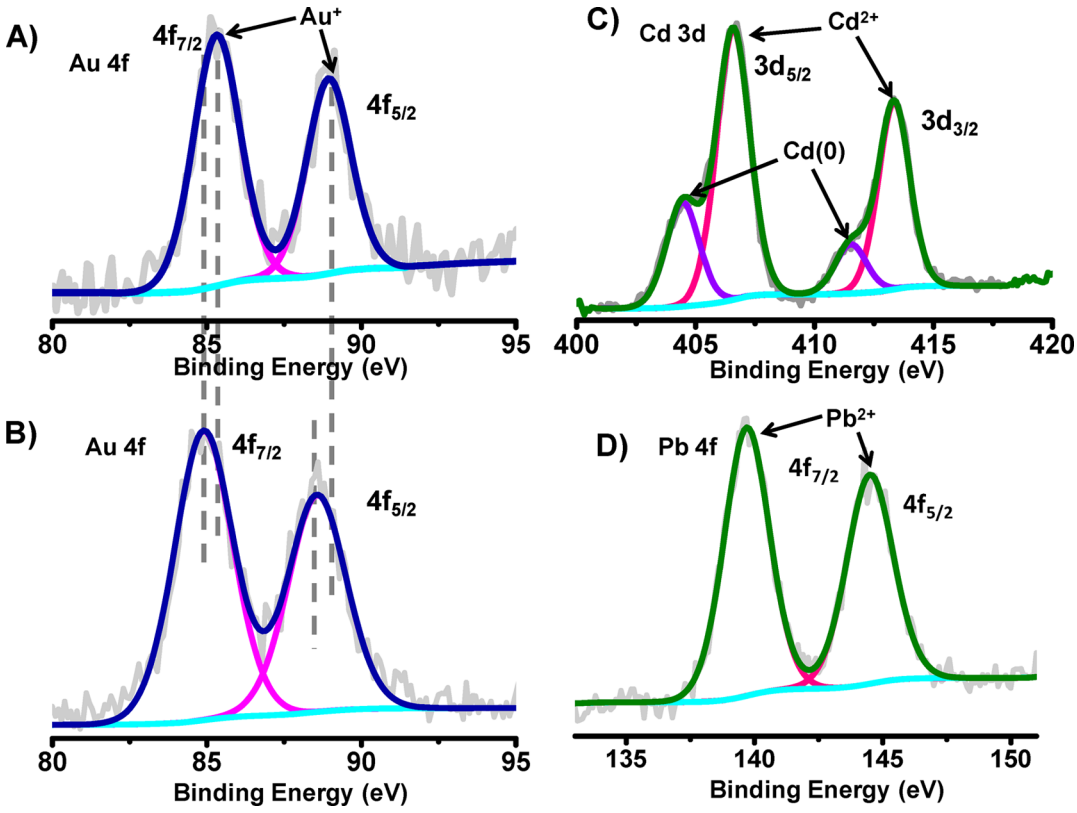

Figure 4. (A and B) Au 4f region of Au_{38}@BSA upon interaction with Cd^{2+} and Pb^{2+}, respectively. (C and D) Corresponding Cd 3d and Pb 4f regions, respectively.

change in the oxidation state of the cluster core, i.e. from Au^0 to Au^+ whereas Pb^{2+} did not bring a significant change in the core of the cluster. This also supported the results obtained from PL studies discussed earlier.

DOI: 10.1021/acs.jpcc.9b07370
J. Phys. Chem. C 2019, 123, 28969−28976

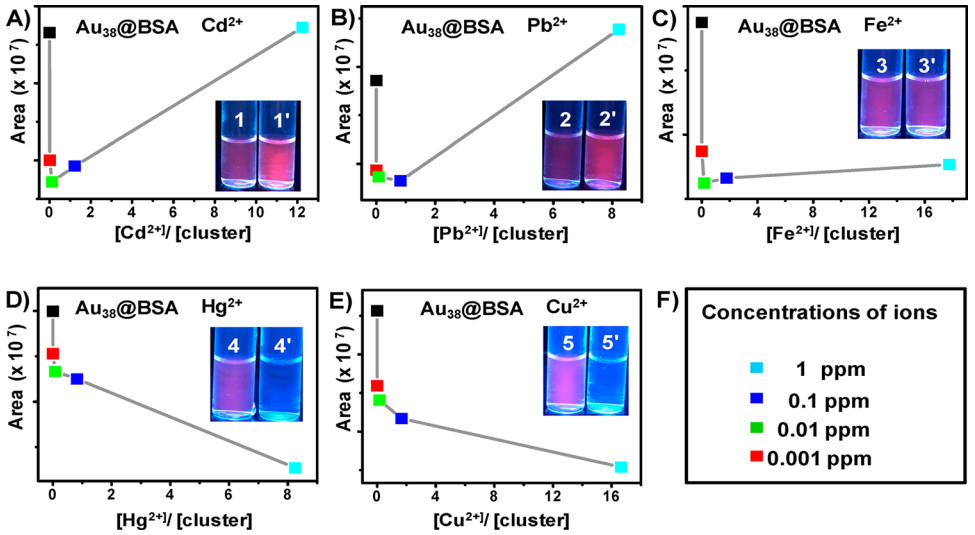

Figure 5. Area under the emission spectra at different molar ratios of metal ions to cluster concentrations. (A) Cd^{2+}, (B) Pb^{2+}, (C) Fe^{2+}, (D) Hg^{2+}, and (E) Cu^{2+}. (F) Color coding for the concentrations of metal ions used. Inset shows the photographs of Au_{38}@BSA before (1, 2, 3, 4, 5) and after interaction with 1 ppm of Cd^{2+}, Pb^{2+}, Fe^{2+}, Hg^{2+}, and Cu^{2+} (1′, 2′, 3′, 4′, 5′), respectively.

Selective Luminescence Enhancement of Au_{38}@BSA Due to Metal Ions. The interactions of Au_{38}@BSA with Cd^{2+} and Pb^{2+} were discussed in the earlier sections and enhancement of luminescence was observed at higher concentrations of Cd^{2+} and Pb^{2+} while luminescence was quenched at lower concentration. The luminescence response of Au_{38}@BSA was studied with other divalent metal ions such as Fe^{2+}, Hg^{2+}, and Cu^{2+}, and the changes were compared with Cd^{2+} and Pb^{2+} ions. Figure 5 shows the change in the luminescence of the cluster after treatment with metal ion concentrations starting from 1 ppb to 1 ppm. Area under the emission spectrum of Au_{38}@BSA (550−710 nm wavelength range) is plotted against the molar ratio of metal ion to Au_{38}@BSA, for different analyte ions.

After addition of each concentration of metal ion to cluster, the cluster solution was incubated for 2 min before collecting the emission spectra. Only in the presence of Cd^{2+} and Pb^{2+}, luminescence enhancement was seen but not in the case of Fe^{2+}. Whereas at lower concentrations of Cd^{2+}, Pb^{2+}, and Fe^{2+}, a decrease in the emission intensity was noticed. Enhancement in emission started from 0.1 ppm of Cd^{2+} and Pb^{2+} onward. In the earliest sections, we have already discussed the effect of increase in the concentration of Cd^{2+} and Pb^{2+} (Figure 2, parts A and C). Unlike Hg^{2+}, Cu^{2+} also is known to quench the luminescence of Au_{QC}@BSA.[13,24] In both cases, at lower concentrations (up to 100 ppb), a decrease in the luminescence intensity was observed, but complete quenching occurred only at 1 ppm of ions. The interaction of Cu^{2+} with BSA shell of the cluster has been proposed as a possible reason for this luminescence quenching, whereas a similar quenching effect in the case of Hg^{2+} is due to the interaction between the metal ion and the core of the cluster.[13,24]

CONCLUSIONS

The interaction of Au_{38}@BSA with Cd^{2+} and Pb^{2+} has been investigated in great detail. Au_{38}@BSA was found to have aggregation-induced emission *enhancement* in the presence of Cd^{2+} and Pb^{2+}, for concentrations higher than 1 ppm. This phenomenon has been studied for the first time in the case of PPCs. The enhancement of luminescence is due to aggregation of clusters, and such aggregates were detected by DLS and HRTEM analyses. PL studies have shown that, in the case of Cd^{2+}, enhancement in the luminescence is due to interaction between Cd^{2+} and cluster core whereas PL enhancement in Au_{38}@BSA upon Pb^{2+} is due to Pb^{2+}−protein shell interaction. These observations were further supported by XPS data, where it was shown that interaction with Cd^{2+} resulted in the oxidation of the cluster core from Au^0 to Au^+ along with changes in binding energy of Cd^{2+}, but interaction of Pb^{2+} did not affect the core of the cluster. Interactions of other metal ions such as Fe^{2+}, Hg^{2+}, and Cu^{2+} with Au_{38}@BSA were also studied and it showed that such interaction is selective to Cd^{2+} and Pb^{2+}. Difference in the nature of interactions between heavy metal ions and Au_{38}@BSA may be used to develop a sensor with a logical readout for identifying different metal ions. Also, such metal-ion-induced aggregation of clusters leading to emission enhancement will open up the possibility of developing clusters with enhanced optical properties and associated applications.

ASSOCIATED CONTENT

Supporting Information

The Supporting Information is available free of charge on the ACS Publications website at DOI: 10.1021/acs.jpcc.9b07370.

Comparative MALDI MS of BSA and ~Au_{38}@BSA, control PL study and time dependent change in I_{650} of Au_{38}@BSA, UV−vis absorption spectra of Au_{38}@BSA in the presence of Cd^{2+} and Pb^{2+}, DLS data, HRTEM EDS spectra, and XPS data of Au_{38}@BSA (PDF)

AUTHOR INFORMATION

Corresponding Author

*(T.P.) E-mail: pradeep@iitm.ac.in. Fax: +91-44-2257-0545.

ORCID

Thalappil Pradeep: 0000-0003-3174-534X

Notes

The authors declare no competing financial interest.

DOI: 10.1021/acs.jpcc.9b07370
J. Phys. Chem. C 2019, 123, 28969−28976

■ ACKNOWLEDGMENTS

We thank the Department of Science and Technology, Government of India for their continuous support on our research program on nanomaterials. J.S.M. thanks Council of Scientific and Industrial Research (CSIR) for her research fellowship. C.S. thanks IIT Madras for his research fellowship.

■ REFERENCES

(1) Jin, R. Quantum Sized, Thiolate-Protected Gold Nanoclusters. *Nanoscale* **2010**, *2*, 343−362.
(2) Mathew, A.; Pradeep, T. Noble Metal Clusters: Applications in Energy, Environment, and Biology. *Part. Part. Syst. Charact.* **2014**, *31*, 1017−1053.
(3) Xavier, P. L.; Chaudhari, K.; Baksi, A.; Pradeep, T. Protein-Protected Luminescent Noble Metal Quantum Clusters: An Emerging Trend in Atomic Cluster Nanoscience. *Nano Rev.* **2012**, *3*, 14767−14782.
(4) Chevrier, D. M.; Chatt, A.; Zhang, P. Properties and Applications of Protein-Stabilized Fluorescent Gold Nanoclusters: Short Review. *J. Nanophotonics* **2012**, *6*, 064504.
(5) Rao, T. U. B.; Nataraju, B.; Pradeep, T. Ag_9 Quantum Cluster through a Solid-State Route. *J. Am. Chem. Soc.* **2010**, *132*, 16304−16307.
(6) Sharma, J.; Rocha, R. C.; Phipps, M. L.; Yeh, H.-C.; Balatsky, K. A.; Vu, D. M.; Shreve, A. P.; Werner, J. H.; Martinez, J. S. A DNA-Templated Fluorescent Silver Nanocluster with Enhanced Stability. *Nanoscale* **2012**, *4*, 4107−4110.
(7) Zheng, J.; Zhang, C.; Dickson, R. M. Highly Fluorescent, Water-Soluble, Size-Tunable Gold Quantum Dots. *Phys. Rev. Lett.* **2004**, *93*, 077402.
(8) Xie, J.; Zheng, Y.; Ying, J. Y. Protein-Directed Synthesis of Highly Fluorescent Gold Nanoclusters. *J. Am. Chem. Soc.* **2009**, *131*, 888−889.
(9) Goswami, N.; Zheng, K.; Xie, J. Bio-NCs - the Marriage of Ultrasmall Metal Nanoclusters with Biomolecules. *Nanoscale* **2014**, *6*, 13328−13347.
(10) Mathew, A.; Sajanlal, P. R.; Pradeep, T. A Fifteen Atom Silver Cluster Confined in Bovine Serum Albumin. *J. Mater. Chem.* **2011**, *21*, 11205−11212.
(11) Li, H.-W.; Ai, K.; Wu, Y. Fluorescence Visual Gel-Separation of Dansylated BSA-Protected Gold-Nanoclusters. *Chem. Commun. (Cambridge, U. K.)* **2011**, *47*, 9852−9854.
(12) Mohanty, J. S.; Xavier, P. L.; Chaudhari, K.; Bootharaju, M. S.; Goswami, N.; Pal, S. K.; Pradeep, T. Luminescent, Bimetallic AuAg Alloy Quantum Clusters in Protein Templates. *Nanoscale* **2012**, *4*, 4255−4262.
(13) Habeeb Muhammed, M. A.; Verma, P. K.; Pal, S. K.; Retnakumari, A.; Koyakutty, M.; Nair, S.; Pradeep, T. Luminescent Quantum Clusters of Gold in Bulk by Albumin-Induced Core Etching of Nanoparticles: Metal Ion Sensing, Metal-Enhanced Luminescence, and Biolabeling. *Chem. - Eur. J.* **2010**, *16*, 10103−10112.
(14) Baksi, A.; Pradeep, T. Noble Metal Alloy Clusters in the Gas Phase Derived from Protein Templates: Unusual Recognition of Palladium by Gold. *Nanoscale* **2013**, *5*, 12245−12254.
(15) Baksi, A.; Pradeep, T.; Yoon, B.; Yannouleas, C.; Landman, U. Bare Clusters Derived from Protein Templates: Au_{25}^+, Au_{38}^+ and Au_{102}^+. *ChemPhysChem* **2013**, *14*, 1272−1282.
(16) Baksi, A.; Xavier, P. L.; Chaudhari, K.; Goswami, N.; Pal, S. K.; Pradeep, T. Protein-Encapsulated Gold Cluster Aggregates: The Case of Lysozyme. *Nanoscale* **2013**, *5*, 2009−2016.
(17) Xavier, P. L.; Chaudhari, K.; Verma, P. K.; Pal, S. K.; Pradeep, T. Luminescent Quantum Clusters of Gold in Transferrin Family Protein, Lactoferrin Exhibiting Fret. *Nanoscale* **2010**, *2*, 2769−2776.
(18) Chaudhari, K.; Xavier, P. L.; Pradeep, T. Understanding the Evolution of Luminescent Gold Quantum Clusters in Protein Templates. *ACS Nano* **2011**, *5*, 8816−8827.
(19) Anand, U.; Ghosh, S.; Mukherjee, S. Toggling between Blue- and Red-Emitting Fluorescent Silver Nanoclusters. *J. Phys. Chem. Lett.* **2012**, *3*, 3605−3609.
(20) Chan, P.-H.; Chen, Y.-C. Human Serum Albumin Stabilized Gold Nanoclusters as Selective Luminescent Probes for Staphylococcus Aureus and Methicillin-Resistant Staphylococcus Aureus. *Anal. Chem. (Washington, DC, U. S.)* **2012**, *84*, 8952−8956.
(21) Liu, C.-L.; et al. Insulin-Directed Synthesis of Fluorescent Gold Nanoclusters: Preservation of Insulin Bioactivity and Versatility in Cell Imaging. *Angew. Chem., Int. Ed.* **2011**, *50*, 7056−7060.
(22) Li, H.; Zhu, W.; Wan, A.; Liu, L. The Mechanism and Application of the Protein-Stabilized Gold Nanocluster Sensing System. *Analyst (Cambridge, U. K.)* **2017**, *142*, 567−581.
(23) Habeeb Muhammed, M. A.; Ramesh, S.; Sinha, S. S.; Pal, S. K.; Pradeep, T. Two Distinct Fluorescent Quantum Clusters of Gold Starting from Metallic Nanoparticles by pH-Dependent Ligand Etching. *Nano Res.* **2008**, *1*, 333−340.
(24) Xie, J.; Zheng, Y.; Ying, J. Y. Highly Selective and Ultrasensitive Detection of Hg^{2+} Based on Fluorescence Quenching of Au Nanoclusters by Hg^{2+}-Au^+ Interactions. *Chem. Commun. (Cambridge, U. K.)* **2010**, *46*, 961−963.
(25) Liu, Y.; Ai, K.; Cheng, X.; Huo, L.; Lu, L. Gold-Nanocluster-Based Fluorescent Sensors for Highly Sensitive and Selective Detection of Cyanide in Water. *Adv. Funct. Mater.* **2010**, *20*, 951−956.
(26) Wei, H.; Wang, Z.; Yang, L.; Tian, S.; Hou, C.; Lu, Y. Lysozyme-Stabilized Gold Fluorescent Cluster: Synthesis and Application as Hg2+ Sensor. *Analyst (Cambridge, U. K.)* **2010**, *135*, 1406−1410.
(27) Mathew, A.; Sajanlal, P. R.; Pradeep, T. Selective Visual Detection of TNT at the Sub-Zeptomole Level. *Angew. Chem., Int. Ed.* **2012**, *51*, 9596−9600.
(28) Chen, T.-H.; Tseng, W.-L. (Lysozyme Type VI)-Stabilized Au_8 Clusters: Synthesis Mechanism and Application for Sensing of Glutathione in a Single Drop of Blood. *Small* **2012**, *8*, 1912−1919.
(29) Shao, C.; Yuan, B.; Wang, H.; Zhou, Q.; Li, Y.; Guan, Y.; Deng, Z. Eggshell Membrane as a Multimodal Solid State Platform for Generating Fluorescent Metal Nanoclusters. *J. Mater. Chem.* **2011**, *21*, 2863−2866.
(30) Li, M.; Yang, D.-P.; Wang, X.; Lu, J.; Cui, D. Mixed Protein-Templated Luminescent Metal Clusters (Au and Pt) for H_2O_2 Sensing. *Nanoscale Res. Lett.* **2013**, *8*, 182.
(31) Chevrier, D. M.; et al. Structure and Formation of Highly Luminescent Protein-Stabilized Gold Clusters. *Chem. Sci.* **2018**, *9*, 2782−2790.
(32) Wang, S.; Meng, X.; Das, A.; Li, T.; Song, Y.; Cao, T.; Zhu, X.; Zhu, M.; Jin, R. A 200-Fold Quantum Yield Boost in the Photoluminescence of Silver-Doped $AgxAu_{25-X}$ Nanoclusters: The 13th Silver Atom Matters. *Angew. Chem., Int. Ed.* **2014**, *53*, 2376−2380.
(33) Mohanty, J. S.; Baksi, A.; Lee, H.; Pradeep, T. Noble Metal Clusters Protected with Mixed Proteins Exhibit Intense Photoluminescence. *RSC Adv.* **2015**, *5*, 48039−48045.
(34) Luo, Z.; Yuan, X.; Yu, Y.; Zhang, Q.; Leong, D. T.; Lee, J. Y.; Xie, J. From Aggregation-Induced Emission of Au(I)-Thiolate Complexes to Ultrabright Au(0)@Au(I)-Thiolate Core-Shell Nanoclusters. *J. Am. Chem. Soc.* **2012**, *134*, 16662−16670.
(35) Ji, L.; Guo, Y.; Hong, S.; Wang, Z.; Wang, K.; Chen, X.; Zhang, J.; Hu, J.; Pei, R. Label-Free Detection of Pb^{2+} Based on Aggregation-Induced Emission Enhancement of Au-Nanoclusters. *RSC Adv.* **2015**, *5*, 36582−36586.
(36) Wu, C.-S.; Cupps, J. M.; Fan, X. Compact Quantum Dot Probes for Rapid and Sensitive DNA Detection Using Highly Efficient Fluorescence Resonant Energy Transfer. *Nanotechnology* **2009**, *20*, 305502.
(37) Todd, M. D.; Lee, M. J.; Williams, J. L.; Nalezny, J. M.; Gee, P.; Benjamin, M. B.; Farr, S. B. The Cat-Tox (L) Assay: A Sensitive and Specific Measure of Stress-Induced Transcription in Transformed Human Liver Cells. *Fundam. Appl. Toxicol.* **1995**, *28*, 118−128.

DOI: 10.1021/acs.jpcc.9b07370
J. Phys. Chem. C 2019, 123, 28969−28976

(38) Brewer, G. J. Risks of Copper and Iron Toxicity During Aging in Humans. *Chem. Res. Toxicol.* **2010**, *23*, 319−326.
(39) Miyake, Y.; et al. MercuryII-Mediated Formation of Thymine-HgII-Thymine Base Pairs in DNA Duplexes. *J. Am. Chem. Soc.* **2006**, *128*, 2172−2173.
(40) Kim, H.-K.; Rasnik, I.; Liu, J.; Ha, T.; Lu, Y. Dissecting Metal Ion-Dependent Folding and Catalysis of a Single DNAzyme. *Nat. Chem. Biol.* **2007**, *3*, 763−768.
(41) Needleman, H. Lead Poisoning. *Annu. Rev. Med.* **2004**, *55*, 209−222.
(42) Hussein, H.; Farag, S.; Kandil, K.; Moawad, H. Tolerance and Uptake of Heavy Metals by Pseudomonads. *Process Biochem. (Oxford, U. K.)* **2005**, *40*, 955−961.
(43) Kunkel, R.; Manahan, S. E. Atomic Absorption Analysis of Strong Heavy Metal Chelating Agents in Water and Waste Water. *Anal. Chem.* **1973**, *45*, 1465−1468.
(44) Ochsenkuhn-Petropoulou, M.; Ochsenkuhn, K. M. Comparison of Inductively Coupled Plasma-Atomic Emission Spectrometry, Anodic Stripping Voltammetry and Instrumental Neutron-Activation Analysis for the Determination of Heavy Metals in Airborne Particulate Matter. *Fresenius' J. Anal. Chem.* **2001**, *369*, 629−632.
(45) Goswami, N.; Giri, A.; Bootharaju, M. S.; Xavier, P. L.; Pradeep, T.; Pal, S. K. Copper Quantum Clusters in Protein Matrix: Potential Sensor of Pb^{2+} Ion. *Anal. Chem. (Washington, DC, U. S.)* **2011**, *83*, 9676−9680.
(46) Saha, K.; Agasti, S. S.; Kim, C.; Li, X.; Rotello, V. M. Gold Nanoparticles in Chemical and Biological Sensing. *Chem. Rev. (Washington, DC, U. S.)* **2012**, *112*, 2739−2779.
(47) Liu, J.; Lu, Y. Preparation of Aptamer-Linked Gold Nanoparticle Purple Aggregates for Colorimetric Sensing of Analytes. *Nat. Protoc.* **2006**, *1*, 246−252.
(48) Liu, J.; Lu, Y. Improving Fluorescent Dnazyme Biosensors by Combining Inter- and Intramolecular Quenchers. *Anal. Chem.* **2003**, *75*, 6666−6672.
(49) Durgadas, C. V.; Sharma, C. P.; Sreenivasan, K. Fluorescent Gold Clusters as Nanosensors for Copper Ions in Live Cells. *Analyst (Cambridge, U. K.)* **2011**, *136*, 933−940.
(50) Baksi, A.; Mitra, A.; Mohanty, J. S.; Lee, H.; De, G.; Pradeep, T. Size Evolution of Protein-Protected Gold Clusters in Solution: A Combined SAXS-MS Investigation. *J. Phys. Chem. C* **2015**, *119*, 2148−2157.

DOI: 10.1021/acs.jpcc.9b07370
J. Phys. Chem. C 2019, 123, 28969−28976